Volume 9, Number 4
1009-1963/2000/09(04)/0284-06
CHINESE PHYSICS
April, 2000
© 2000 Chin. Phys. Soc.

CHARACTERIZATION OF POLYCRYSTALLINE GRADIENT THIN FILM BY X-RAY DIFFRACTION METHOD*

Li Bin(李 彬), Tao Kun(陶 琨), Liu Xing-tao(刘兴涛),
Miao Wei(苗 伟), Feng Tao(冯 涛), Yang Ning(杨 宁),
and Liu Bai-xin(柳百新)

Department of Materials Science and Engineering, Tsinghua University, Beijing 100084, *China*

(Received 22 August 1999)

A direct method is proposed to quantitatively characterize the structural depth profiles emerged in the polycrystalline thin films based on the information obtained by X-ray diffraction (XRD) with various incident angles and treated by a numerical procedure known as the constrained linear inversion. It should be noted that the proposed method was neither sensitive to the random noise appearing in experiment nor to the error originated from the measured thickness of the specimen. To testify the validity of the method, XRD measurements were carried out on a specially designed Pd/Ag bilayer sample, which was annealed at 490 ℃ for 20 min, and the depth profiles were accordingly calculated through resolving the obtained XRD patterns. The elemental concentration depth profile of the Pd/Ag bilayer sample was in turn calculated from the resolved patterns, which was in good agreement with those obtained by Auger electron analysis on the annealed sample.

PACC: 6110F; 6822; 0650

I. INTRODUCTION

Study of sample surfaces and thin films is a growing and important application of the X-ray diffraction (XRD) technique. Considerable effort has been directed to the characterization of surface and thin films over the past decades. For the polycrystalline thin films, some methods were presented to obtain the depth profiles emerged in the thin films by XRD.[1−9] In this respect, however, since the analysis process is a typical ill-posed inverse problem in mathematics, to develop a method retrieving the real depth profile directly and quantitatively has been somewhat difficult.

We report, in this paper, the principle of a proposed method to directly obtain the structure depth profiles emerged in the thin films featuring gradient structure. The main effort was to overcome the above mentioned problems. The proposed method was testified by comparing the calculated depth profiles of a specially designed Pd/Ag bilayer sample after thermal annealing with those obtained by Auger measurements.

II. PRINCIPLE

The fundamental principle of depth profiling can be found in some previously published literature.[10−14] Briefly, based on our previous works, the present method, namely the asymmetrical diffraction method was used to measure the diffraction patterns and the layout of the method is shown in Fig.1.[10,11] For a thin film sample with preferred orientation, the diffraction ability of each infinitesimal thin layer at depth x is represented by $I(x,\theta,\boldsymbol{S})$, where the vector $\boldsymbol{S}$ is the normal to the diffraction plane in the sample. As to the diffraction scheme shown in Fig.1, the sample rotates around the axis $\boldsymbol{S}$

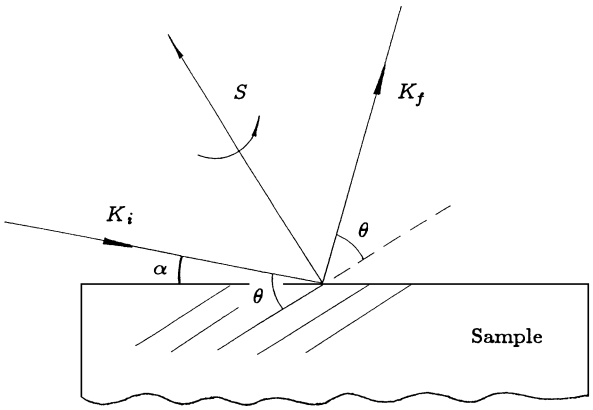


Fig.1. Asymmetrical Bragg diffraction scheme. The sample is rotated around axis $\boldsymbol{S}$.

and in this way the variation of the rotation angle corresponds to the change of the incident angle. Consequently, the grains with the same orientation are measured when the incident angle varies. The formulae of ZRD intensity can therefore be expressed as[11,12]

$$I_{\rm obs}(\phi,\theta\boldsymbol{S}) = A(\phi,\theta,\boldsymbol{S})\cdot\int_0^\infty I(x,\theta,\boldsymbol{S})\cdot\exp(-\sigma Y)\mathrm{d}x, \quad (1)$$

* Project supported by the National Natural Science Foundation of China (Grant No. 59471066).

and

$$Y = Y(x) = \int_0^x \mu(x)\mathrm{d}x, \tag{2}$$

$$\begin{aligned}\sigma =& \sigma(\phi,\theta,\boldsymbol{S}) = 1/[\cos(\theta-\alpha_0)\sin\theta \\ & - \cos\theta\cos\phi\sin(\theta-\alpha_0)] + 1/[\cos(\theta \\ & - \alpha_0)\sin\theta + \cos\theta\cos\phi\sin(\theta-\alpha_0)],\end{aligned} \tag{3}$$

where σ is the diffraction geometrical factor for the preferred orientation samples. α_0 is the original incident angle while the plane defined by $\boldsymbol{K_i}$ and $\boldsymbol{K_f}$ is perpendicular to the sample surface; ϕ is defined as the rotation angle when the sample rotates around the vector $\boldsymbol{S}$ from the original position. $I_{\mathrm{obs}}(\phi,\theta,\boldsymbol{S})$ is the diffraction pattern obtained from the experiment, $\mu(x)$ is a linear absorption coefficient of the thin layer at an arbitrary depth x. The factor $A(\phi,\theta,\boldsymbol{S})$ can be obtained from the measurement of a calibration sample. The $Y(x)$, which is defined as the absorption depth, can be used as a depth scale directly.[10−12] To obtain $I(x,\theta,\boldsymbol{S})$, i.e. the diffraction ability at depth x or the structure information depth profile, Eq.(1) is transformed into

$$I^*_{\mathrm{obs}}(\sigma) = \int_0^D I^*(Y)\cdot\exp(-\sigma Y)\mathrm{d}Y, \tag{4}$$

where $I^*_{\mathrm{obs}} = I_{\mathrm{obs}}/A$, $I^*(Y) = I(Y(x))/\mu(x)$. D is the total thickness of the thin film in absorption depth Y. If the substrate contributes mostly to the formation of the background intensity, or it contributes little to the net intensity of the diffraction peak, D should be used in Eq.(4) instead of infinite thickness. To resolve Eq.(4), the constrained linear inversion method was employed in this ill-posed inverse problem.

Assuming the function $I^*(Y)$ is bounded and continuous in the depth range considered, it can be expressed approximately by a piece-wise linear function[12−14]

$$I^*(Y) = \sum_{k=1}^{N} I^*_k \cdot C_k(Y),$$

where

$$C_k(Y) = \begin{cases} (Y - Y_{k-1})/(Y_k - Y_{k-1}), & Y_{k-1} \le Y \le Y_k, \\ (Y_{k+1} - Y)/(Y_{k+1} - Y_k), & Y_k \le Y \le Y_{k+1}, \\ 0, & \text{elsewhere}, \end{cases} \tag{5}$$

where N is the total number of the divided layers, and the coefficients I^*_k are the heights of $I^*(Y)$ at abscissa values Y_k in the absorption depth scale. Substituting Eq.(5) into Eq.(4) for each measured intensity $[\sigma_i, I^*_{\mathrm{obs}}(\sigma_i)]$, where $i = 1, 2, \cdots M$, and M is the total number of the measured patterns, leads to a final result

$$[\boldsymbol{C}]\{\boldsymbol{a}\} = \{\boldsymbol{b}\}, \tag{6}$$

where $C_{ik} = \int_0^D C_k(Y)\cdot\exp(-\sigma_i Y)\mathrm{d}Y$, $a_k = I^*_k$, and $b_i = I^*_{\mathrm{obs}}(\sigma_i)$. The solution of Eq.(6) is obtained by the constrained linear inversion method as follows[12,13]

$$\{\boldsymbol{a}\} = (\boldsymbol{C}^T\boldsymbol{C} + \beta\boldsymbol{H})^{-1}C^T\{\boldsymbol{b}\}, \tag{7}$$

and the matrix of linear constraint is

$$H = \begin{bmatrix} 1 & -1 & 0 & \cdots & \cdots & \cdots & 0 \\ -1 & 2 & -1 & \cdots & \cdots & \cdots & 0 \\ 0 & -1 & 2 & \cdots & \cdots & \cdots & 0 \\ \cdots & \cdots & \cdots & \cdots & \cdots & \cdots & \cdots \\ 0 & \cdots & \cdots & \cdots & 2 & -1 & 0 \\ 0 & \cdots & \cdots & \cdots & -1 & 2 & -1 \\ 0 & \cdots & \cdots & \cdots & 0 & -1 & 1 \end{bmatrix}_{N\times N}.$$

Here β represents the relative weight of the linear constraint term, which must be adjusted to obtain a reasonable solution for the function $I^*(Y)$. The choice of β is actually a trade-off between resolution and stability of the numerical inversion process.

The resulting function $I^*(Y)$ can therefore be obtained, and it represents the diffraction pattern in the label of the absorption depth Y. The absorption depth Y can also be used as a depth scale and its characteristics resemble the sputtering time in Auger electron spectroscopy(AES) sputter depth profiling analysis.[11] If the linear absorption coefficient $\mu(x)$ is a constant, Y will be proportional to the real depth. Generally, the concentration of the existing phases in each analyzed layer can be computed from the resolved patterns. The $\mu(x)$ and the structure depth profiling in real depth scale can thus be calculated.

Ⅲ. EXPERIMENTAL PROCEDURE

A Pd(200 nm)/Ag(200 nm) bilayer was prepared by depositing Pd and Ag onto a SiO_2/Si(100) substrate under a base vacuum of 1.3×10^{-6} Pa. The SiO_2 layer on the Si surface was used to prevent the reaction between Si and the Pd/Ag bilayer. The bilayer sample was annealed at 490 ℃ for 20 min. Since the Pd-Ag system is essentially of a complete solid solution type, interdiffusion would take place in the bilayer during thermal annealing, resulting in the formation of Pd-Ag solid solutions, of which the lattice parameters changed gradually along the depth.

The XRD measurement was performed with a diffractometer D/max-rB with Cu $K\alpha$ radiation. The

automatic sample holder was made to accord with the asymmetric Bragg diffraction scheme shown in Fig.1. Parallel beam method was employed in the analysis. In the measurement the (111) peak lines of the bilayer film were used. In the step scanning the step width of the diffraction angle $\Delta 2\theta$ was 0.02°, and the counting time was 1 second. The angle α_0 in Eq.(3) is 1°. Twenty rotation angles ϕ corresponding to twenty incident angles from 1° to about 16° were used to collect 20 original patterns, i.e. M=20. The tested sample was divided into twenty analyzing layers using the scale of absorption depth, i.e. N=20. The proposed method was executed to calculate the diffraction ability.

IV. RESULTS

A. Testing with designated profiles

To test the accuracy of the numerical procedure, the following diffraction ability profiles $I^*(Y)$ were designated:

$$\begin{aligned} I_1^*(Y) &= \exp(-2Y/D) \times 80000, \\ I_2^*(Y) &= (1 - \exp(-2Y/D)) \times 80000 + 20000, \\ I_3^*(Y) &= \begin{cases} 80000, & Y \le D/2 \\ 20000, & Y > D/2 \end{cases} \end{aligned} \tag{8}$$

where D is 0.095, determined by Rutherford back scattering(RBS) experiment of the sample. These functions have different line shapes, which provide useful information for testing the sensitivity and validity of the numerical procedure. In Eq.(7), $\alpha_0 = 1°, \phi = 0°, 2°, 4°, 6°, 9°, 12°, 15°, 18°, 21°, 25°, 30°, 35°, 40°, 45°, 50°, 55°, 60°, 70°, 80°, 90°$, M=N=20; and twenty data points at $2\theta = 40°$ were employed in the testing process.

In the test, the diffraction intensity profiles $I^*_{\rm obs}(\sigma)$ were firstly calculated according to Eq.(6), and then a random error was added to the calculated intensity profiles. By the present method, the calculated diffraction ability profiles $I^*_{\rm c}(Y)$ were retrieved according to Eq.(7). The deviation of these two profiles was defined as

$$\eta_{\rm err} = \sqrt{\sum_{i=1}^{N}(I^*_{ci} - I^*_i)^2} \Big/ \sqrt{\sum_{i=1}^{N} I^{*2}_i}, \tag{9}$$

where I^*_{ci} and I^*_i are respectively data points of profiles $I^*_{\rm c}(Y)$ and $I^*(Y)$ at the ith layer. By the comparison of the retrieved profiles $I^*_{\rm c}(Y)$ and the initial given profiles $I^*(Y)$, or by the shape of the error lines and the values $\eta_{\rm err}$, the retrieved effects of the method were clearly shown.

Figure 2 shows the retrieved effects on profile $I^*_1(Y)$ for the cases that different random noises were added to the calculated $I^*_{\rm obs}(\sigma)$. In Figs.2(a) and 2(b) the random noises are ±5% and ±10%, respectively. It was found that to allow a reasonable retrieval effect, different random noises required different suitable constraint term β, and the present method functioned well under the condition of at least ±10% random noises. Moreover, the larger the random noise

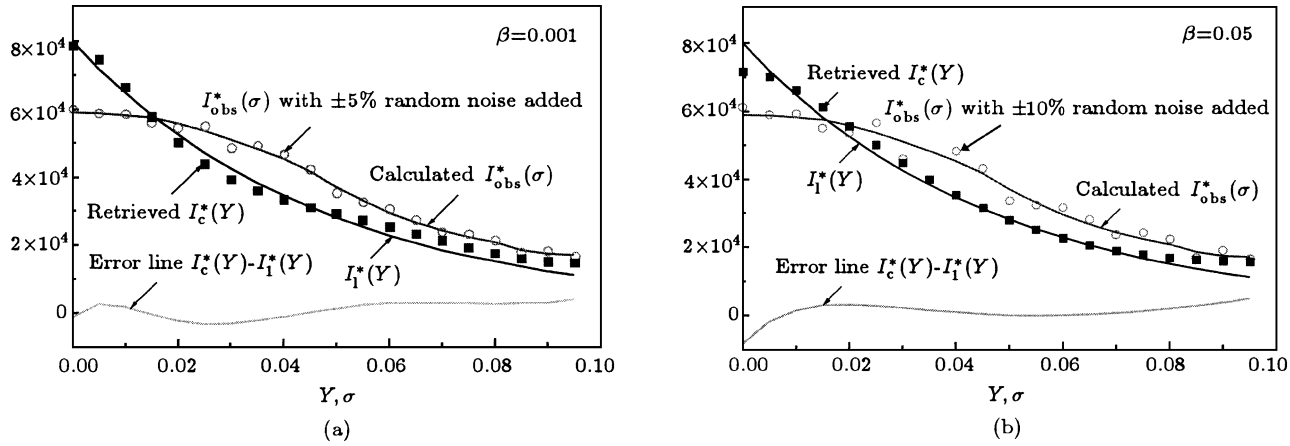


Fig.2. Testing the procedure on known intensity ability profile $I^*_1(Y)$. The unit of the ordinate is arbitrary. (a) For the calculated $I^*_{\rm obs}(\sigma)$ to which a ±5% random noise is added, the deviation $\eta_{\rm err}$ is 5.9%. (b) For the calculated $I^*_{\rm obs}(\sigma)$ to which a ±10% random noise is added, the deviation $\eta_{\rm err}$ is 6.8%.

added on the calculated $I^*_{\rm obs}(\sigma)$, the bigger the constraint term β, indicating that larger noise needs more smoothing or constraint. In Fig.3, it can be seen that different constraint terms β result in different retrieval effects. As shown in Fig.3(a), if β is too small to constraint, the resulting $I^*_{\rm c}(Y)$ tends to be sensitive to the quality of $I^*_{\rm obs}(\sigma)$ and will be oscillatory. On the other hand, if β is too big in constraint, the result would be very stiff and the retrieved profile $I^*_{\rm c}(Y)$ will be close to a straight line. In Fig.3(b), it is shown that the range of suitable β is relatively large, within which the retrieval effect changes very slightly, ensuring a relatively flexible choice of β.

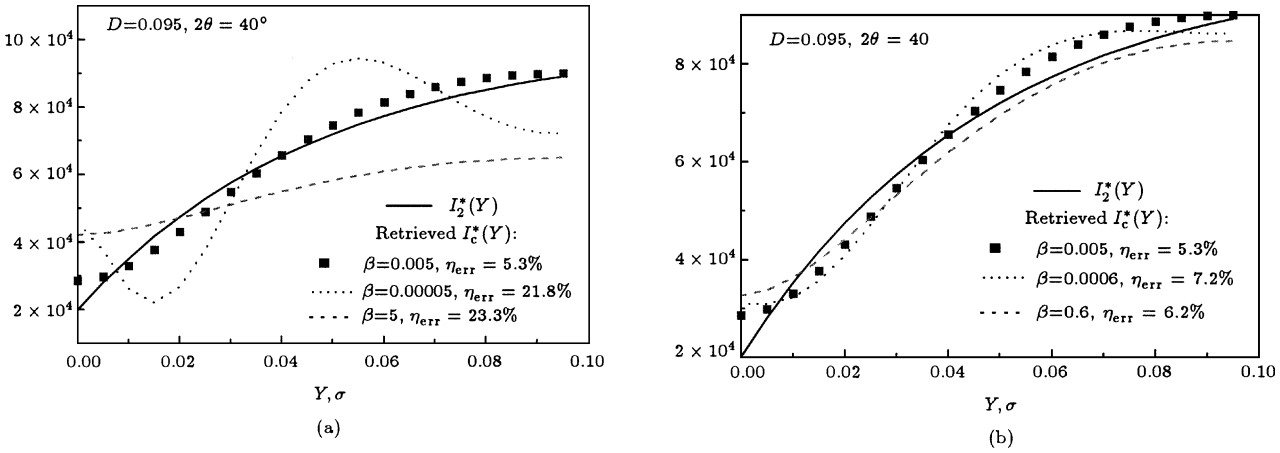


Fig.3. Testing the procedure on designated intensity ability profile $I^*_2(Y)$ with different linear constraint term β. $A \pm 5\%$ random noise is introduced to the calculated $I^*_{\rm obs}(\sigma)$, and the unit of the ordinate is arbitrary. (a) In case that β is too large or too small, the resulting retrieved $I^*_{\rm c}(Y)$ is either oscillatory or stiff. (b) The range of the suitable β to obtain a reasonable retrieval is relatively large.

For thin films, the film thickness may not be known exactly and the total absorption depth D is probably uncertain either. Figure 4 shows that in the case of adding 20% error to D, i.e. D=0.114 and a $\pm$5% random noise is added to $I^*_{\rm obs}(\sigma)$, the retrieved profile is also in good accordance with the given profile. The above discussion indicates that the method is not sensitive to D.

As shown above, the method was applicable to the gradient profiles, as shown in Figs.2–4. In the computing procedure, it has been found that a suitable value of β should be as small as possible in the case that no oscillation happens in the retrieved profile. Moreover, the retrieval effect changes very slightly within a relatively large range of suitable β.

However, this method is invalid for samples of stepwise structure profile due to the influence of the constraint term β. As shown in Fig.5, though no error is introduced into the calculated $I^*_{\rm obs}(\sigma)$, the retrieval effect is far from satisfactory, no matter what value of β is. It is therefore concluded that the method is not applicable to the sample with sharp interface.

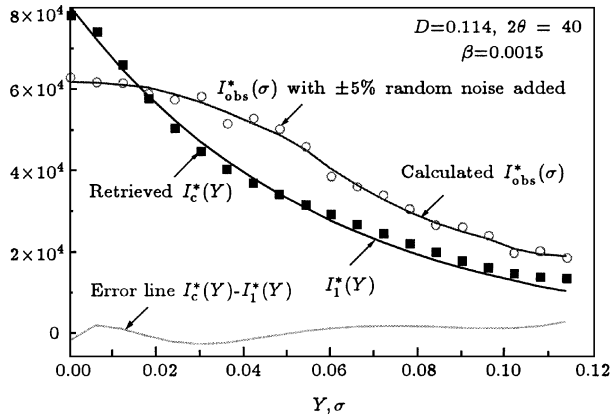


Fig.4. Testing the procedure on designed profile $I^*_1(Y)$ with a 20% error added to D and a $\pm$5% random noise added to $I^*_{\rm obs}(\sigma)$. The unit of the ordinate is arbitrary. The deviation $\eta_{\rm err}$ is 8.1%.

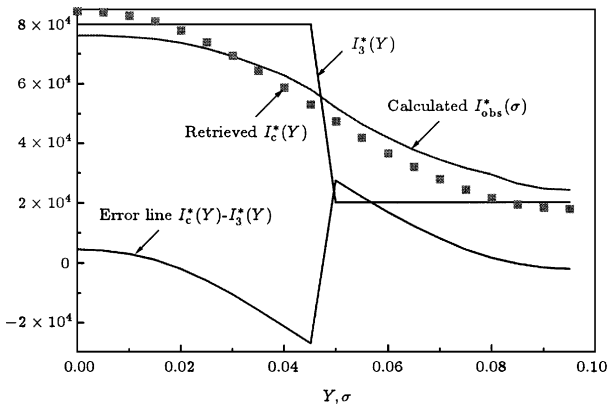


Fig.5. Testing the procedure on known profile $I^*_3(Y)$. The unit of the ordinate is arbitrary. D is 0.095 and 2θ is 40°. No random noise is added to the calculated $I^*_{\rm obs}(\sigma)$. The deviation $\eta_{\rm err}$ is 22.2%.

B. Application to the measured intensity profiles

The original intensity patterns measured by the asymmetric method are shown in Fig.6. The X-ray

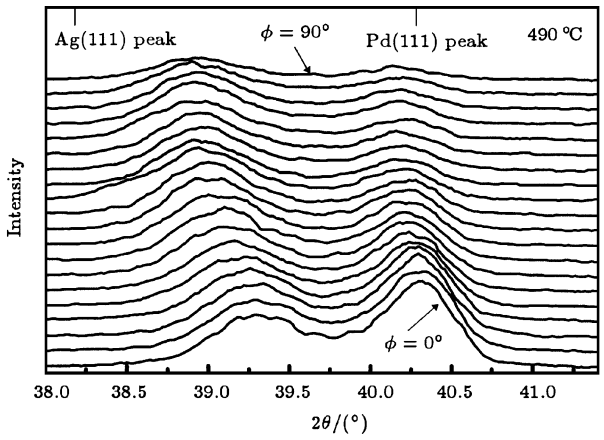


Fig.6. The measured XRD patterns of the Pd/Ag bilayer sample annealed at 490 ℃ for 20 min. The rotation angle ϕ increases from 0° to 90° for these measured patterns, and the information depths of the patterns increase from 70 nm to 1 μm.

information depth of the measurement was controlled by varying the rotation angle, ϕ, and it ranged from 70 nm to 1 μm. It can be shown that there were interdiffusion between the surface layer of Pd and the inner layer of Ag in the annealed sample. Figure 7 shows the computed patterns of each thin layer of the tested sample by the present method. It should be noted that the resolving process was performed along depth for each 2θ point, separately, and then the computed patterns of each layer were plotted instantly without any data smoothing. In the computed procedure, a common constraint term β for all the $I^*(Y)$ data along 2θ points was determined to allow just no oscillation and no negative points in each resolved profile. In Fig.7, the constraint term β is 8.0, which is an appropriate value.

From Fig.7, it can be shown that there are two solid solutions with different lattice parameters in each layer at different depth, indicating that the structure of each layer parallel to the surface is not homogeneous microscopically. Besides, with the increase of depth, the position shift of the Pd(111) peak is smaller than that of the Ag(111) peak, and the intensity of it decreases more obviously than that of the Ag(111) peak. This is due to the fact that it is easier for Pd to diffuse into Ag to form Pd→Ag solid solution than for Ag to pervade into Pd to form Ag→Pd solution.

As shown in Fig.7, the computed patterns are continuous, smooth and neat so that they can provide some detailed and precise structure information. Furthermore, the linear absorption coefficient of Pd(2290/cm) is very close to that of Ag(2470/cm), therefore the absorption depth Y is approximately proportional to the real depth. Consequently, each resolved pattern in Fig.7 reflects the real structure information of each layer of 20nm thickness. Comparatively, in Fig.6 the measured patterns only reflect the information depth profiles of the sample surface about 1 μm thickness.

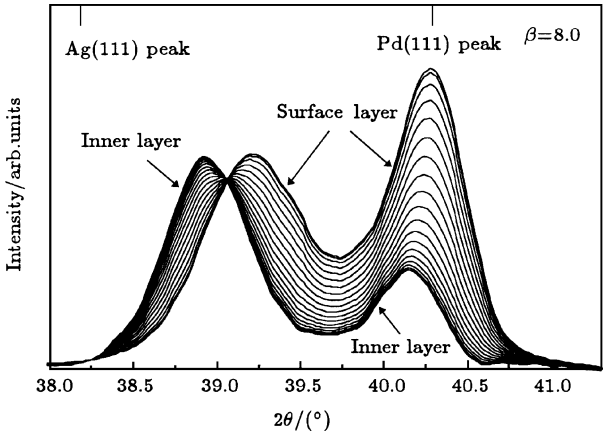


Fig.7. Results of the structure depth profiling for Pd/Ag bilayer sample annealed at 490 ℃ for 20 min. The computed patterns correspond to the absorption depth Y increasing homogeneously from 0.005 to 0.1, in which $M = N$ =20, D=0.1 and β=8.0.

V. DISCUSSION

According to the Vegard's Law, and the integral intensity ratio of the two peaks after peak separation, which corresponds to the content ratio of the two solid solutions, the elemental concentration of each layer was calculated from the computed patterns in Fig.7 and is shown in Fig.8(a). AES experiment combined with Ar^+ ion sputtering was performed to directly obtain the elemental depth profile of the tested sample. The sputtering rate measured for pure Pd was 2.0 nm/min and the resulting pattern is shown in Fig.8(b). By the comparison of Figs.8(a) and 8(b), it can be seen that the calculated depth profile is in good agreement with that obtained by the Auger electron measurement, confirming the validity of the proposed structure depth profiling method.

VI. CONCLUSIONS

We have proposed a method for direct characterization of the structure depth profiles in the polycrystalline thin films. The method was employed in calculating the real structure depth profiles of a specially

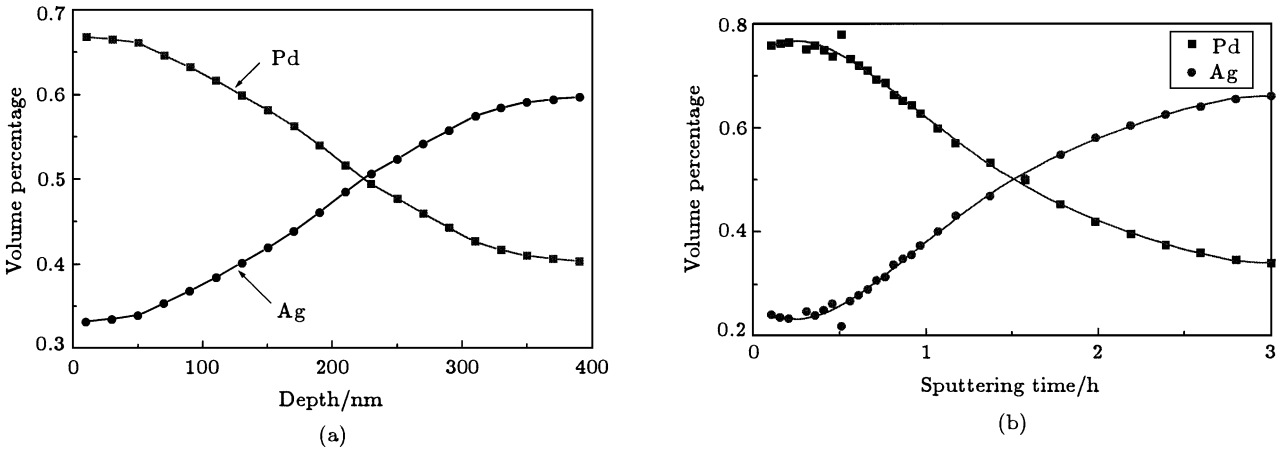


Fig.8. The elemental depth profiles of the tested sample obtained by the proposed XRD method and AES analysis, respectively. (a) The calculated elemental depth profile of the tested sample according to Fig.7. (b) AES elemental depth profile of the tested sample.

designed Pd/Ag bilayer sample, which was thermally annealed to form Pd-Ag solid solutions with different lattice constants along the depth. The concentration depth profiles calculated by using the proposed method are in good agreement with those from AES analysis. It is noted that the numerical algorithm employed in this study is more effective for the gradient structure than for the case with sharp interfaces. Moreover, the present method is more suitable for analyzing those samples with weak preferred orientation than those of strong texture.

REFERENCES

[1] C. R. Houska, *J. Appl. Phys.*, **41**(1970), 69.
[2] M. F. Doerner and S. Brennan, *J. Appl. Phys.*, **63**(1988), 126.
[3] Q. Z. Cong, D. Y. Yu , L. J. Wen and F. Q. Zhang, *Thin Solid Films*, **213**(1992), 13.
[4] T. C. Huang, *Adv. X-Ray Anal.*, **33**(1990), 91.
[5] A. V. Riessen and B. H. Oconnor, *Adv. X-Ray. Anal.*, **35**(1992), 169.
[6] M. F. Toney, T. C. Huang, S. Brennan and Z. Rek, *J. Mater. Res.*, **3**(1988), 351.
[7] Q. Z. Cong, *J. Appl. Cryst.*, **25**(1992), 582.
[8] T. Kosaka, S. Suzuki, H. Inoue, M. Saito, Y. Waseda and E. Matsubara, *Appl. Surf. Sci.*, **103**(1996), 55.
[9] X. de Buchere, P. Andreazza, C. Andreazza-Vignolle, C. Clinard and R. Erre, *Surf. Coat. Tech.*, **80**(1996), 49.
[10] J. Luo and K. Tao, *Acta Physica Sinica*, **44**(1995), 1793(in Chinese).
[11] J. Luo and K. Tao, *Thin Solid Films*, **279**(1996), 53.
[12] K. Tao, B. Li and J. Luo, *Acta Metallurgica Sinica*, **33**(1997), 51(in Chinese).
[13] X. J. Zhu, B. Ballard and P. Predecki, report presented at the Denver X-ray Conference, Steamboat Springs, Colorda, August 1-5, 1994.
[14] J. Luo, K. Tao, H. Yin and Y. Du, *Rev. Sci. Instrum.*, **67**(1996), 2859.